23rd ABCM International Congress of Mechanical Engineering
December 6-11, 2015, Rio de Janeiro, RJ, Brazil

THE ELIMINATION OF EXCESSIVE VIBRATION PRESENTED BY ALTITUDE SIMULATION TEST FACILITY FOR LOW THRUST ROCKET ENGINES.

Roman Ivanovitch Savonov
José Nivaldo Hinckel
INPE-Nasional Institute For Space Researtc, Av.dos Astronautas, 1758, Jd. Granja – CEP:12227-010, São José dos Campos, Brasil.
romansav@lcp.inpe.br
jose.hinckel@inpe.br

Aguinaldo Martins Serra Júnior
INPE-Nasional Institute For Space Researtc, Av.dos Astronautas, 1758, Jd. Granja – CEP:12227-010, São José dos Campos, Brasil.
agnaldo@lcp.inpe.br

Abstract. *The Altitude Simulation Test Facility (ASTF) is directed to carry out tests of low thrust rocket engines (from 2 up to 20 N). ASTF should allow performing measurement of various features and parameters of the thrusters (chamber pressure, mass flow rate of propellants, thrust, etc.) with high precision. Many tests of the thrusters have been performed on this test facility, but for some, the thrust measurement showed high amplitude oscillations. The amplitude of these oscillations on some test instants exceeded the real value of the engine force by 70-100%. It implicates on an adequate analysis of the principal characteristics of the rocket thrusters. The modal analysis of the system was performed to detect the origin of vibration. Introduction of the viscous damper in the dynamical scheme of the test facility system was proposed as the solution of the problem. The optimization analysis of the damping value was performed, and, the damper project and manufacturing was realized. The final test was carried out to compare the response of the initial and modified system.*

Keywords: *test facility, vibration, thruster, damper.*

1. INTRODUCTION

Low thrust liquid engines are used in propulsion systems of satellites, spacecraft, space stations, missiles and ballistic rockets. Its principal functions are attitude control, correction of satellite orbit, accuracy orientation and apogee insertion. Monopropellant low thrust liquid engines utilizing hydrazine as propellant are widely used in this field due the simple design and propulsive characteristics. Design of these thrusters does not include an ignition system. This factor permits the utilization of the thrusters in a pulsed mode and increase accuracy in the control maneuvers. But on the other hand, the pulsed mode may result in decrease an efficiency of the thruster, particularly when the time between pulses is relatively long. Study of the thrust control of hydrazine rocket motor with minimization of the efficiency lose was presented by Hanan and Alon (1991).

Monopropellant rocket engines may present thrust oscillation during operation, like the solid, liquid and hybrid rocket engines. These oscillations are the result of interactions between the acoustic pressure and the combusting process in the case of the solid, liquid and hybrid rocket engines. The study of the high-, intermediate-, and low-frequency combustion instability in solid rocket engine is presented by Price (1965). Richecoeur *et. al.*(2006) experimentally investigated in model scale research facility high-frequency instabilities in liquid propellant rocket engine and reveal flame structure modification for specific injection condition correspond to a strong coupling between acoustic and combustion that notably modify the flow dynamics, augments the flame expansion rate and enhances heat transfer to the wall. Kyung-Su and Changjin (2015) presented the work with experimental test designed to examine the triggering mechanism of low-frequency instability in the hybrid rocket engines, which occurred at a certain combustion condition. In the monopropellant rocket engines this oscillation occurred due the differences of the local pressure in the catalytic bed during the decomposition process. These oscillations are usually observed during the transition regime between catalytic and thermal decomposition.

The oscillation of the chamber pressure during propellant decomposition, pulsed regime of operation and others sources of periodical excitation force create the difficult measurement problems in test of the low thrust engines because its amplitude may pass 50% of the average thrust of the engine. The low thrust engines are destined to be used in the space condition with lowered external pressure and must be tested on the particular test facilities. General description of the systems of this type test facilities can be find in (Ellerbrock and Ziegenhagen 2006).

2. ELIMINATION OF VIBRATIONS ON THE TEST FACILITY.

3. Description of the test facility and determination of the dynamical model.

The *ASTF* utilized by National Institute for Space Research (INPE), is presented on the Fig. (1). This facility is designed to test the monopropellant hydrazine thrusters with thrust from 2 up to 20 N.

a). b).

Figure 1. Altitude Simulation Test Facility.

The facility consists of the five principal subsystems: vacuum subsystem, propellant subsystem and utilities, support and test balance, electrical command and control data acquisition subsystem and safety. The vacuum subsystem has pumps and vacuum chamber with support and thrust balance. The thrust balance is connected with force cell and fixed on the support, which, in turn, fixed on the lower part of the vacuum chamber as shown on Fig. (1. b). During operation of the test facility the pumps are activated by electrical motors to produce vacuum condition inside the chamber. The seismic block, for isolation the chamber from external excitation force, was not provided in the test facility project, and oscillation may pass from motors to chamber by foundation and affect the data read by acquisition system from force cell.

An initial series of test was performed to measure and analyses the influence of the electrical motor on the force cell response. Figure 2 present the result of these tests.

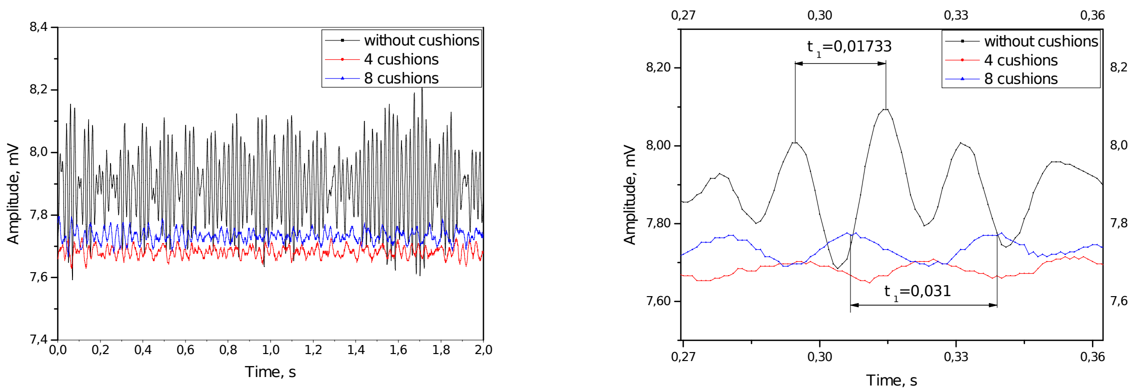

Figure 2. Electrical motor influence on the force cell response.

The black line on Fig. 2.b shows data captured from force cell during operating of the electrical motors when balance support was fixed on the chamber body directly. The blue line matches the data of the test, when four cushions were introduced between support and chamber, one for the each support foot. And the red line presents the case with eight cushions (two on the each foot of the support, for isolation of screw and nut fixation). The decrement of vibration is very noticeably in the cases of the system with cushions.

The period of oscillation of the system without cushions is τ*=0,0173 s*, according Fig.2.b, and, consequently its frequency is:

$$\omega_1 = \frac{1}{\tau_1} = \frac{1}{0{,}01733} = 57{,}7\,Hz$$

The frequency of the motor rotation is 56,7 Hz (3400 rpm) is very close to the frequency of the system oscillations without cushions. In this case, oscillations pass from motors to force cell in the form of an external harmonic force, and, if its frequency will be close to fundamental frequency of the system, may induce vibrations with high amplitude. In the two other cases, the frequency of the vibrations is very different, and passes to system as random no periodic force. The amplitude of the system vibrations is very small due of dumping by cushions. The interference of these vibrations on the force cell response during test can be neglected. The isolation of the system from external force with utilizing of the cushions is satisfactory.

The second part of this work is prevention of possible vibration that may be a result of periodic oscillation of the engines thrust to be tested. There are two possible sources of this oscillation – the pulsed mod operation of the thruster and thrust oscillations due to the decomposition process of propellant. The problem of this vibration can be solved numerically or mechanically, modifying dynamical scheme of the system by utilizing damping element or specific force cell. Lin *et al.*, 2015 proposed a practical compensation method for the measurement system using left inverse model as numerical solution. Xing *et al.*, 2010 developed a novel thrust dynamometer with high fundamental frequency for accurately measuring the pulsed thrust. The disadvantage of this method is decrease of the measurement accuracy with variation of the thruster mass in the case of the test different engines. Our proposal is the utilization of a viscous damper to decrease the vibration and achieve necessary accuracy of measurement data. First, the dynamical model of the system must be determined. The scheme of the system is present on Fig.3.

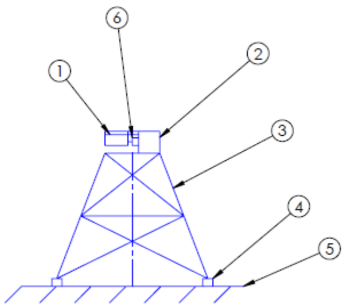

Figure 3. Scheme of the balance with support.

The thrust balance support consists of the base (position 2), truss (position 3). The truss fixed on the chamber body (position 5) by screw connection. The cushions (position 4) are situated between chamber body and truss. The base is fixed on the truss by welding connection. The thrust balance (position 1) is connected to the base through force cell (position 6). The system was excited by knock on the three different parts (truss, base and chamber body).The response on the force cell is present on the Fig. 4.

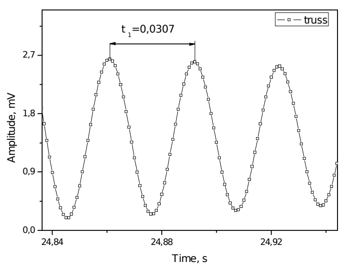

exited on truss

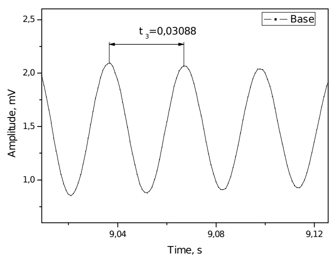

exited on base

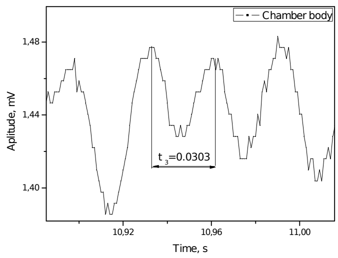

exited on chamber body
Figure 4. Free vibrations of the system

Periods, and, consequently, frequencies of the free vibration of the system in three cases are very close to each other. This test shows that the set (truss, base and chamber body) can be presented as a single body in the dynamic model.

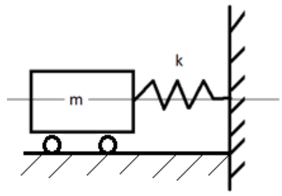

Figure 5. Dynamic model of the system.

The dynamic model of the system is simple and includes one mass element and stiffness. Mass element (*m*) presents the mass of balance and *k* is stiffness of the force cell.

Now we need to determine the optimum value of damping constant of the system. The dumping constant must be critical, to ensure aperiodic motion and the mass returns to the position of rest in the shortest possible time without overshooting. If the damping provided is higher than the critical value, some delay would be caused. Value of the damping will confine the period of the pulses during test of the thrusters. Critical value of the damping can be determined following Rao (2009) as:

$$c_c = 2\sqrt{km} \tag{1}$$

Where *k* – stiffness of the force cell; *m* – mass of the balance.

The values of the *k* and *m* are unknown for our system. First, we need to find the value of the fundamental frequency. Free vibration of the system was analyzed for this purpose.

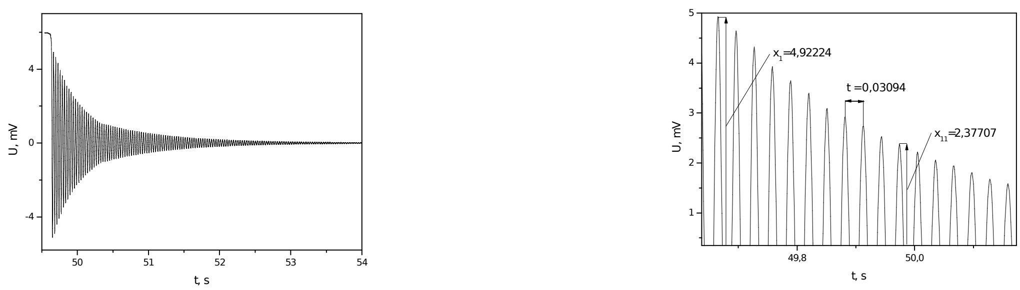

a) b)

Figure 6. Free vibrations of the system.

Figure (6) shows free vibration of the system. This vibration is underdamped (Fig. 6.a) with hysteretic dumping, because no damper was used. Fundamental frequency of the system is calculated as:

$$\omega_n = \frac{\omega_d}{\sqrt{1 - \zeta^2}} \tag{2}$$

where ω_d - frequency of the dumped system, ζ- damping ratio.

Damping ratio is calculated using logarithmic decrement:

$$\zeta = \frac{\delta}{\sqrt{(2\pi)^2 + \delta^2}} \tag{3}$$

And logarithmic decrement is found as:

$$\delta = \frac{1}{m} \ln\left(\frac{X_1}{X_{m+1}} \right) \tag{4}$$

Where m – number of the cycle, X_1 and X_{m+1} – amplitude of the first and last cycle respectively.

In accordance with (Fig.6.b) $m=10;\ X_1=4{,}92; X_{11}=2{,}37;\ \tau_d=0{,}0309$. Substituting these values into Eq.(4) we obtain: $\delta=0{,}073$, next $\zeta=0{,}01162$ and $\omega_n=207{,}076$ *(rad/s).*
Equation of motion of the underdamped system is:

$$x(t) = e^{-\zeta\omega_n t}\left\{ x_0 \cos\sqrt{1-\zeta^2}\,\omega_n t + \frac{\dot{x}_0 + \zeta\omega_n x_0}{\sqrt{1-\zeta^2}\,\omega_n} sen\sqrt{1-\zeta^2}\,\omega_n t \right\} \tag{5}$$

Substituting obtained values into (Eq.5), and taking $x_0=5$, $\dot{x}_0 = 0$ we find equation of motion of our system:

$$x(t) = e^{-2{,}406t}\{5\cos(207{,}076t) + 0{,}0581 sen(207{,}076t)\} \tag{6}$$

Figure 7 present comparison of the analytical curve with test data.

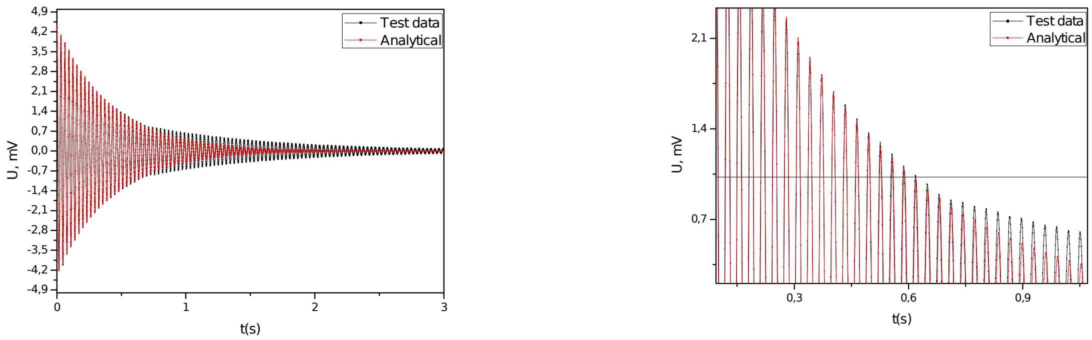

a). b).

Figure 7. Comparison of the analytical solution with test data.

Analytical solution is identical to the test data in the range where displacement of the force cell spring matches values of the force from 1N to 5N, and then values of the frequency and other parameters are correct. The curves differ from each other to force values less than 1N, because the load cell is calibrated to measuring force in the range from 1N to 20N. Out of this range stiffness of the cell becomes no-linear and measurement is inaccurate.

Next, the mass of balance was modified by adding a mass of 0,5 kg, and fundamental frequency was calculated for this system. This procedure permits compose the system of equation to find the m and k.

$$\begin{cases} \omega_1^2 = k/m \\ \omega_2^2 = k/(m+m_1) \end{cases} \tag{7}$$

Where ω_1 and ω_2 – frequencies of the system; k – stiffness of the force cell; m – balance mass; $m_1=0{,}5\ kg$ (adding mass).

Solving Eq. (7) we obtain $m=1{,}187(\ kg)$ and $k=50905\ (N/m)$.

2.2. Choice of the optimal damping constant and project of the damper. Comparison of the results.

Now, all principal parameters of the system are known, and optimum value of the damping constant can be found.

Mass of the system during test of the different thrusters varies, because the thrusters have different mass. The value of the dumping constant may be estimate by two ways: a). on the balance can be fixed some weight with sum of mass equal mass of the greatest thruster, hence during the test of any thruster, takes of some weight from balance, so that the sum of mass of the remaining weights with mass of the thruster continues equal initial mass of the system; b). damping constant can be calculated for the system with intermediate mass. Disadvantage of the first way is rise of the time that the system needs to return in the rest position. Disadvantage of the second way is system operation out of critical damping condition. The solutions were evaluated with purpose to choose best of them.

Figure (8) presents system behavior for various cases of solution.

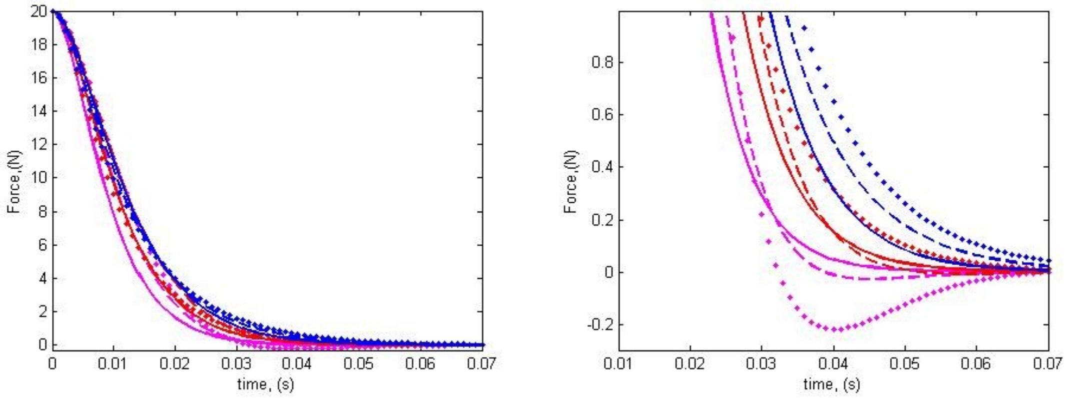

Figure 8. Behavior of the system for different mass and damping constant.

The pink solid curves show the system response with critical damping constant for mass *m=1,187* (kg) (empty balance); the dashed pink curve matches the system with same damping constant, but with adding the mass of 0,5 (kg) (balance + thruster (0,5 kg)), and doted curve – same damper , and adding mass of thruster 1 (kg). The critical time of the system with this damper is 0,037 s. The system is underdamped in two last cases.

All red curves present system with critical damping calculated for the intermediate mass *m=1,687* (kg), hence the solid curve – critically damped system, dashed curve – underdamped system (*m= 2,187* kg), doted curve – overdamped system (*m-1,187* kg).

The blue curves match the response of the system with critical damping constant calculated for the mass *m=2,187* kg. The system is underdamped in two other cases (*m=1,687* kg and *m=1,187* kg).

The analysis of the curves shows, that using the underdamped system (pink doted line) is more profitable, because the dynamic error is negligible and response time of the system is smallest. Hence, the damping constant is calculating for system with parameters: *m=1,187(kg)* and *k=50905 (N/m).* Substituting these values into Eq. (1) obtain:

$$c_c = 2\sqrt{50905{,}88 \cdot 1{,}187} = 491{,}63 \frac{Ns}{m}$$

The principal dimensions of the dashpot with this damping constant can be calculated according following equation (Rao, 2009)

$$c = \mu\left[\frac{3\pi D^3 l}{4d^3}\left(1+\frac{2d}{D}\right)\right] \tag{8}$$

Where c – damping coefficient; μ – viscosity; D – diameter of the piston; d – clearance between piston and cylinder, l – length of the piston.

The dashpot, with dimensions: D = 21 (mm); d = 0,5 (mm); l = 8 (mm), was designed, and tested on the test facility.

Figure (8) presents the comparison of the system without damper, system with designed damper and analytical curve of the critically damped system.

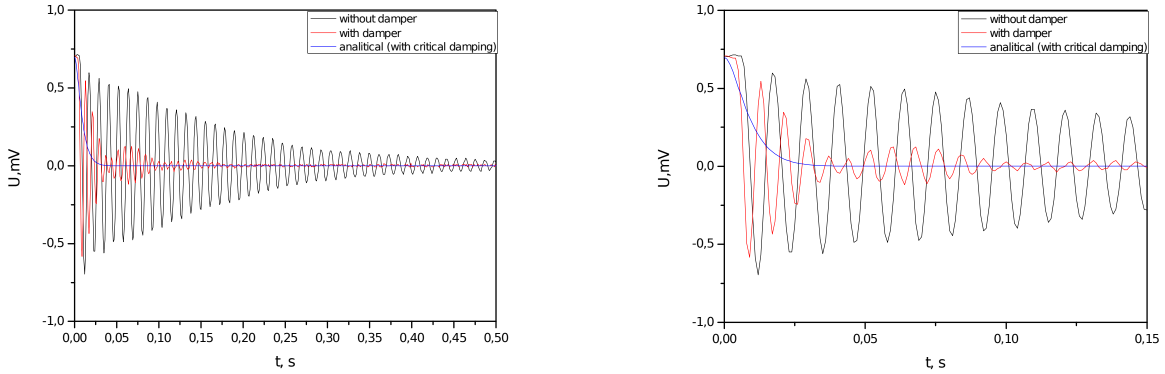

a). b).

Figure 9. Comparison of the undamped, damped and critically damped system.

The red curve presents the behavior of the system with designed damper. The decay of the amplitude of vibrations for this case is five times faster compared with original system. It is a good result for first attempt at problem solving, but on the other hand, is still far from the desired result, presented by blue curve. System continues vibrating for a short time after excitation, because of some unforeseen details in damper design. For example: the oil supply system of damper was not designed correctly. Some volume of air remained inside the damper after supplying, for this reason, the system has second wave of vibrations before stopping. It begins on 0, 045 s and stop on 0,1 s (see Fig. 9. b). It occurs because, the piston, after dislocation, compresses the air. This volume of compressed air acts as an oscillation external force and interacts with spring of the force cell, and system oscillates until it comes into equilibrium. We also can observe that the red curve presents the motion of the underdamped system. The damping constant of the designed damper is less then critical. The clearance between the piston and the cylinder of the manufactured damper is larger than theoretical calculated value.

2.3. Conclusions.

The realized work showed that viscous damper can be successfully applied on the thrust measuring subsystem to reduce vibrations. The result of the tests enabled to understand the physical behavior of the system. The manufacturing precision of the damper should be improved. The system of oil supply should be provided to avoid the air presence inside the damper. The dynamical essay with external oscillation load should be realized on the future work to guarantee the precision in measurements of the thrust of the rocket engines.

4. REFERENCES

Ellerbrock, H. and Ziegenhagen, S., 2006. “Liquid rocket engine test facility engineering challenges”. *Acta Astronautica*, Vol. 59, p. 1123 – 1134.

Lin,C., Jie, C. and Jianxun, L., 2015. “Practical compensation for nonlinear dynamics thrust measurement system”. *Chinese Journal of Aeronautics*, Vol. 28. No.1, pp. 418–426.

Richecoeur, F., Ducruix, S., Scouflaire, P., Candel,S.,2008. “Experimental investigation of high-frequency combustion instabilities in liquid rocket engine”. *Acta Astronautica*. Vol. 62,pp. 18 – 27.

Park, K., Lee C., 2015.” Low frequency instability in laboratory-scale hybrid rocket motors”. *Aerospace Science and Technology*. Vol. 42, pp. 148–157.

Xing, Q., Zhang, J., Qian, M., Jia, C., Sun, B., 2011. “Design, calibration and error analysis of a piezoelectric thrust dynamometer for small thrust liquid pulsed rocket engines”. *Measurement*. Vol. 44, pp. 338–344

Rom, H. and Gany, A., 1992. “Thrust control of hydrazine rocket motors by means of pulse width modulation”. *Acta Astronautica.* Vol. 26., No. 5., pp. 313-316.

Price, E., 1965. “Experimental solid rocket combustion instability”. *Tenth International Symposium on combustion. The Combustion Institute.* Pp. 1067 – 1082.

Rao, S., 2009. *Vibrações mecânicas*. Pearson Education do Brasil. São Paulo. 4ª edição.

5. RESPONSIBILITY NOTICE

The authors are the only responsible for the printed material included in this paper.